Sensors and Actuators B 253 (2017) 630–640

Contents lists available at ScienceDirect

Sensors and Actuators B: Chemical

journal homepage: www.elsevier.com/locate/snb

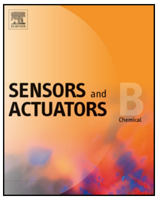

Semiconductor-type SnO_2-based NO_2 sensors operated at room temperature under UV-light irradiation

Takeo Hyodo*, Kaoru Urata, Kai Kamada, Taro Ueda, Yasuhiro Shimizu

Graduate School of Engineering, Nagasaki University, 1-14 Bunkyo-machi, Nagasaki 852-8521, Japan

ARTICLE INFO

Article history:
Received 2 February 2017
Received in revised form 13 June 2017
Accepted 22 June 2017
Available online 29 June 2017

Keywords:
NO_2 sensor
UV-light irradiation
Tin dioxide
Noble metal
Room temperature

ABSTRACT

NO_2-sensing properties of typical oxide (SnO_2, In_2O_3, or WO_3)-based semiconductor gas sensors were measured at 30 °C with and without UV-light irradiation (main wavelength: 365 nm), and effects of noble-metal (Pd or Pt) loading, UV-light intensity (0–134 mW cm^{-2}) and relative humidity in target gas (0–80%RH) on their NO_2-sensing properties were investigated in this study. The UV-light irradiation effectively reduced the resistances of all sensors, enhanced their NO_2 responses in some cases, and tended to accelerate their response and recovery speeds in dry air, because the UV-light irradiation promoted the adsorption and desorption of NO_2-species on the surface. The SnO_2 sensor showed the largest NO_2 response in dry air, among all the pristine oxide sensors, especially under weak UV-light irradiation ($\leq$35 mW cm^{-2}), together with relatively fast response and recovery speeds. The Pd or Pt loading onto SnO_2 enhanced the NO_2 response of the SnO_2 sensor and accelerated their response and recovery speeds in dry air, while XPS analysis indicated that most of the Pd and Pt nanoparticles loaded on the surface were oxidized after heat treatment at 500 °C. Among all the sensors, the 0.05 wt% Pd-loaded SnO_2 sensor showed the largest NO_2 response under weak UV-light irradiation ($\leq$35 mW cm^{-2}), together with relatively fast response and recovery speeds. The addition of moisture to the target gas had adverse effects on the NO_2 responses and the response speeds of the SnO_2 and 0.05 wt% Pd-loaded SnO_2 sensors, but the weak UV-light irradiation (7 mW cm^{-2}) largely reduced the dependence of the NO_2 response of the *0.05*Pd/SnO_2 sensor on relative humidity while maintaining the large NO_2 response, probably because the weak UV-light irradiation promotes the desorption of physisorbed water molecules and then the effective adsorption of NO_2 on the *0.05*Pd/SnO_2 surface.

1. Introduction

Nitrogen dioxides (NO_2), one of the gaseous air pollutants in modern society, are emitted in large amounts from various fossil-fuel combustion systems operated at elevated temperatures. Not only does NO_2 cause negative impacts on human health (e.g., an increase in respiratory symptoms and a reduction in pulmonic function) directly [1,2], but also it reacts with water-based chemicals in the atmosphere to form acid rain causing severe environmental destruction [3]. In addition, NO_2 reacts also with various chemicals (e.g., volatile organic compounds) in the atmosphere under sunlight irradiation, to form other air pollutants such as suspended particulate matters and photochemical oxidants such as ozone, aldehydes, and peroxyacetyl nitrates, and these products also gave a serious risk to human health [4,5]. Therefore, numerous efforts have been so far directed to developing various types of NO_2-sensing devices such as solid electrochemical [6–8], optical [9,10], and acoustic sensors [11,12]. Among them, it is well known that semiconductor gas sensors show relatively large sensitivity and excellent selectivity to NO_2 at elevated temperatures, and SnO_2 [13–16], In_2O_3 [17–19], WO_3 [20–23], and the related materials are especially promising candidates as the NO_2-sensing materials, among all the oxide semiconductors. However, the operation of these semiconductor gas sensors at elevated temperatures causes sintering among oxide particles and the grain growth involved, leading to reduction in the NO_2 sensitivity. The UV and/or visible-light irradiation to the semiconductor gas sensors is one of attractive approaches to solving such problems, because it can reduce the sensor resistance to allow the semiconductor gas sensors to operate even at room temperature (RT). Therefore, NO_2-sensing properties of the semiconductor gas sensors (e.g., SnO_2 [24–26], In_2O_3 [27,28], WO_3 [29]) under UV and/or visible-light irradiation have been recently reported by many researchers, to

---

* Corresponding author at: Graduate School of Science and Technology, Nagasaki University, 1-14 Bunkyo-machi, Nagasaki 852-8521, Japan.
E-mail address: hyodo@nagasaki-u.ac.jp (T. Hyodo).

http://dx.doi.org/10.1016/j.snb.2017.06.155

improve the disadvantages of the operation at elevated temperatures. We also have already demonstrated that UV-light irradiation (main wavelength: 365 nm) enhanced NO_2-sensing properties of SnO_2-based sensors at RT and the Pd loading onto SnO_2 which was prepared by a hydrothermal method improved their NO_2-sensing properties at RT under UV-light irradiation [30–32]. In this study, differences in NO_2-sensing properties between SnO_2, In_2O_3, and WO_3 sensors with and without UV-light irradiation and effects of the UV-light intensity on their NO_2-sensing properties were first examined at 30 °C in air. In addition, impacts of the amount of Pd or Pt loading mainly onto the SnO_2 surface and the amount of moisture (i.e., humidity) in target gas on their NO_2-sensing properties were systematically investigated at 30 °C in air.

2. Experimental

2.1. Preparation of SnO_2, In_2O_3, and WO_3 powders and loading of Pd or Pt onto their oxide surface

SnO_2 powder was prepared according to the following procedure. An appropriate amount of NH_4HCO_3 aqueous solution ($1.0\,mol\,dm^{-3}$) was added into $SnCl_4$ aqueous solution ($1.0\,mol\,dm^{-3}$). The obtained white precipitate was repeatedly centrifuged at a speed of 4500 rpm for 20 min and washed with pure water, and then dried at 100 °C for 18 h in ambient air. The resultant powder was calcined at 600 °C for 1 h in ambient air, to obtain SnO_2 powder. It was confirmed that the crystal structure of the prepared powder was tetragonal SnO_2 (JCPDS No. 41−1445) by X-ray diffraction (XRD) analysis (Rigaku Corp., RINT2200) using Cu Kα radiation (40 kV, 36 mA). In_2O_3 powder, of which crystal structure was assigned to cubic (JCPDS No. 6−416) by XRD analysis, was prepared by pyrolyzing $In(NO_3)_3$, which was dissolved in pure water, and followed by calcination at 600 °C for 1 h in ambient air. WO_3 powder was prepared according to the following procedure. An appropriate amount of HNO_3 aqueous solution ($0.8\,mol\,dm^{-3}$) was added into $NaWO_4$ aqueous solution ($0.15\,mol\,dm^{-3}$). The yellow resultant precipitate was repeatedly centrifuged at a speed of 4500 rpm for 20 min and washed with pure water, and then dried at 100 °C for 18 h in ambient air. The resultant powder was calcined at 500 °C for 2 h in ambient air, to obtain WO_3 powder. It was confirmed that the crystal structure of the prepared powder was monoclinic WO_3 (JCPDS No. 43−1035) by XRD analysis. Specific surface area of the SnO_2, In_2O_3, or WO_3 powder obtained, which was measured by the Brunauer–Emmett–Teller (BET) method using N_2 adsorption-desorption isotherms (Micromeritics Instrument Corp., Tristar3000), was 21.2, 23.7, or 12.0 $m^2\,g^{-1}$, respectively.

In some cases, Pd or Pt nanoparticles were loaded onto the surface of these oxide powders. After an appropriate amount of oxide powders was added into $Pd(NO_3)_2$ or $PtCl_4$ aqueous solution ($0.75\,mol\,dm^{-3}$) and then they were ultrasonicated at RT for 1 h, they were evaporated to dryness at 100 °C for 2 h in air. The resultant solids were heat-treated at 200 °C for 2 h in H_2 to obtain metallic nanoparticles on the oxide surface. The obtained oxide powders loaded with noble metal (N) were denoted as nN/MO [n: amount of noble metal (N: Pd or Pt), 0.03–0.10 (wt%)]. Specific surface area of the nN/MO powders obtained was hardly influenced by the loading of the noble-metal nanoparticles (e.g., specific surface area of *0.05*Pd/SnO_2 powder: ca. 21.0 $m^2\,g^{-1}$), because the amount of noble-metal loading onto the oxide surface was really small ($\leq$0.10 wt%).

Chemical states of the noble metal (Pd or Pt) on the surface of representative nN/MO powders were characterized by X-ray photoelectron spectroscopy using Mg Kα radiation (XPS, Kratos, ACIS-TLATRA DLD), and the binding energy was calibrated using the C 1s level (285.0 eV) from usual contamination. Optical properties of representative oxide powders (SnO_2 and *0.05*Pd/SnO_2) were investigated by ultraviolet (UV)–visible (Vis) spectrophotometer (JASCO Corp., V-650) with an integrated sphere (JASCO Corp., ISV-722).

2.2. Fabrication of thick film sensors and measurement of their gas-sensing properties

Thick film sensors were fabricated by screen printing employing the paste of each oxide powder on an alumina substrate equipped with a pair of interdigitated Pt electrodes (gap size: ca. 500 μm), followed by calcination at 500 °C for 1 h in ambient air. The top-view photograph of a representative sensor element, *0.05*Pd/SnO_2 sensor, is shown in Fig. 1(a). A thick film sensor was set in a test chamber with a temperature-controlled stage (Lincam Scientific Instr., LST420), which was connected with gas-flow system, and gas responses of these sensors were measured to 5 ppm NO_2 balanced with dry or wet (relative humidity (RH): 20–80%) air at 30 °C at a flow rate of $100\,cm^3\,min^{-1}$ under UV-light irradiation by using light-emitting diode (UV-LED, Asahi Spectra Co., Ltd., POT-365, main wavelength: 365 nm, irradiation intensity: $0.8–134\,mW\,cm^{-2}$), after pre-heat treatment at 200 °C for several tens of minutes in dry or wet air. The experimental setup for gas-sensing measurements under UV-light irradiation is shown in Fig. 1(b). The magnitude of response to NO_2 was defined as the ratio (R_{NO_2}/R_a) of sensor resistance in NO_2 balanced with air (R_{NO_2}) to that in air (R_a). The l% response time ($T_{RS}(l)$) were defined as a period necessary to reach l% value of the resistance change ($\log R_{NO_2} - \log R_a$) from the logarithm of sensor resistance in a base gas ($\log R_a$) to that in NO_2 balanced with air ($\log R_{NO_2}$, generally after 15 min from the injection of NO_2 in air). The m% recovery time ($T_{RC}(m)$) were defined as a period necessary to reach $(100 - m)$% value of the resistance change ($\log R_{NO_2} - \log R_a$) after the injection of NO_2 in air was stopped. The response and recovery times contain a delay period from the gas-switching time to the response- and recovery-starting times, ca. 1.2 min, in this study, since the dead volume of the gas-flow pathway and the chamber in the measurement apparatus is ca. 106 cm^3.

3. Results and discussion

3.1. NO_2-sensing properties of unloaded oxide sensors under UV-light irradiation

Fig. 2 shows response transients of a SnO_2 sensor to 5 ppm NO_2 in dry air at 30 °C under different UV-light irradiation intensities. Response transients of In_2O_3 and WO_3 sensors to 5 ppm NO_2 in dry air at 30 °C under different UV-light irradiation intensities were also shown in Fig. S1, and variations in their responses (R_{NO_2}/R_a) to 5 ppm NO_2, resistances in dry air (R_a), and 90% response and 10% recovery times ($T_{RS}(90)$ and $T_{RC}(10)$, respectively) with UV-light intensity were summarized in Fig. 3. In addition, typical sensing characteristics of these sensors were shown in Table 1. The resistance of the SnO_2 sensor under no UV-light irradiation was relatively large in dry air (R_a: ca. $2.5 \times 10^5\,\Omega$), since SnO_2 was a typical n-type semiconducting oxide and the density of electron carriers was relatively low at 30 °C [13–15,24,25,30–32]. In addition, the SnO_2 sensor showed a large positive NO_2 response (ca. 81) under no UV-light irradiation. The behavior indicates that a large amount of NO_2 molecules negatively chemisorbed as NO_2^- on the SnO_2 surface, trapping electron from the SnO_2 bulk [13–15]. However, the response speed was really slow ($T_{RS}(90)$: ca. 12 min) and the sensor showed little recovery behavior ($T_{RC}(10)$: ca. 30 min). Weak UV-light irradiation abruptly decreased the resistance of the SnO_2 sensor in dry air (e.g., R_a: ca. $1.2 \times 10^4\,\Omega$ at $7\,mW\,cm^{-2}$)